



Piezoelectric PZT MEMS technologies for small-scale robotics and RF applications

Jeffrey S. Pulskamp, Ronald G. Polcawich, Ryan Q. Rudy, Sarah S. Bedair, Robert M. Proie, Tony Ivanov, and Gabriel L. Smith

Thin-film piezoelectric lead zirconate titanate (PZT) is one of the most efficient electromechanical coupling transducer materials currently available for microelectromechanical systems (MEMS). This article reviews piezoelectric MEMS (piezo MEMS) technologies using PZT thin films in radio frequency (RF) devices for communications and radar applications and in the emerging field of millimeter-scale robotics. The electromechanical material properties of thin-film PZT uniquely enable insect-inspired and insect-scale autonomous robots. Recent progress on large force and displacement actuators for robotic leg joints, compact and high torque ultrasonic motors, and bioinspired millimeter-scale flapping wing platforms will be presented. The use of thin-film PZT to achieve high performance and low-voltage RF MEMS switches, ultralow power consumption nanomechanical logic circuits, and high coupling and low loss resonators, filters, and transformers are also reviewed.

Introduction

Lead zirconate titanate (PZT) is a versatile material that possesses piezoelectric, pyroelectric, ferroelectric, and electrostrictive material properties. Since the early development of PZT in the 1950s, the material has become pervasive in a variety of bulk actuator applications and is used in low cost ceramic filters due to its piezoelectric properties.[1,2] It has been explored for infrared radiation (IR) detectors and imagers by utilizing its pyroelectric properties.[3] Commercially available ferroelectric random access memory (FRAM) technology based on thin-film PZT exploits its ferroelectric properties for non-volatile memory.[4–7] However, it is the strong piezoelectric properties of thin-film PZT as exploited in piezoelectric MEMS (piezo MEMS) devices that enable exciting new application spaces such as millimeter-scale robotics.

Purely polar piezoelectric (non-ferroelectric) materials such as AlN and ZnO have been extensively explored in MEMS for sensor and resonator applications[8] (as described in the article by Piazza et al. in this issue). Both materials are directly complementary metal oxide semiconductor (CMOS) process compatible and possess low dielectric constants and low material losses, but modest piezoelectric properties. The commercially successful film bulk acoustic resonator filter technology that resides in most cell phones today relies on thin-film AlN as the piezoelectric transducer material.[9,10] In contrast, PZT materials, especially near the morphotropic phase boundary composition (Zr/Ti = 52/48), where the phase transitions between the tetragonal and rhombohedral ferroelectric phases possess higher dielectric constants and higher mechanical and dielectric losses, also exhibit piezoelectric coefficients and electromechanical coupling factors that are more than an order of magnitude larger than those of the non-ferroelectric materials.[11,12] Randomly oriented PZT films exhibit effective thin-film, transverse piezoelectric coefficients $e_{31,f}$ in the range of –6 to –8 C/m^2,[10] while 001 textured films with minimal Zr/Ti gradients through the film thickness have recently shown values as high as –18 C/m^2.[13]

Jeffrey S. Pulskamp, US Army Research Laboratory, Adelphi, MD; Jeffrey.s.pulskamp.civ@mail.mil
Ronald G. Polcawich, US Army Research Laboratory, Adelphi, MD; Ronald.g.polcawich@us.army.mil
Ryan Q. Rudy, University of Maryland, College Park; ryanrudy@umd.edu
Sarah S. Bedair, US Army Research Laboratory, Adelphi, MD; sarah.s.bedair.civ@mail.mil
Robert M. Proie, US Army Research Laboratory, Adelphi, MD; robert.m.proie.civ@mail.mil
Tony Ivanov, US Army Research Laboratory, Adelphi, MD
Gabriel L. Smith, US Army Research Laboratory, Adelphi, MD; Gabriel.l.smith.civ@mail.mil
DOI: 10.1557/mrs.2012.269

© 2012 Materials Research Society
https://doi.org/10.1557/mrs.2012.269 Published online by Cambridge University Press

Piezoelectric actuator properties scale favorably at micron-scale dimensions; actuator force scales with thickness, while flexural stiffness scales with the cube of thickness. This scaling and the high $e_{31,f}$ of PZT enables piezo MEMS actuators that can achieve very large displacements and/or forces. Furthermore, dc power consumption or power efficiency of piezoelectric actuators is largely determined by the dielectric loss of the material. PZT films typically exhibit dielectric loss values less than 5%, leading to extremely power efficient actuators with low leakage currents. PZT thin films permit the application of large electric fields (~75–500 kV/cm) while allowing MEMS devices to operate with near CMOS-compatible voltages. For transducer and resonator applications, the quasi-static electromechanical coupling factors are key material properties.[14] These describe the efficiency with which energy is transduced from one energy domain to another. Applications such as filtering certain cell phone bands can require large coupling factors to achieve the needed filter bandwidth. PZT possesses coupling factors that are far larger than those of AlN and ZnO, and hence can achieve much wider bandwidth filters.

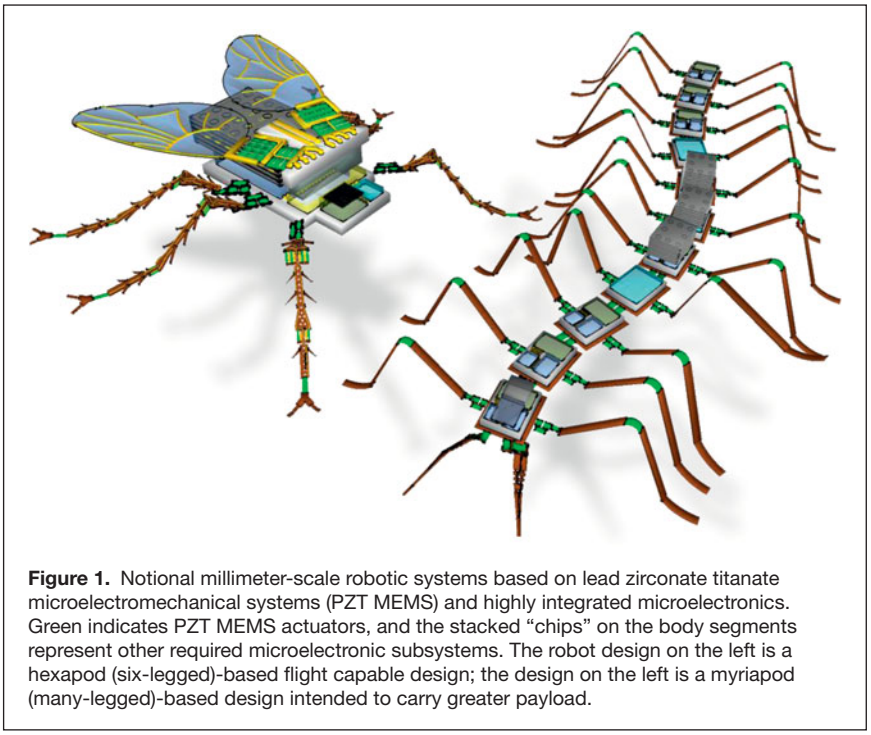


Figure 1. Notional millimeter-scale robotic systems based on lead zirconate titanate microelectromechanical systems (PZT MEMS) and highly integrated microelectronics. Green indicates PZT MEMS actuators, and the stacked "chips" on the body segments represent other required microelectronic subsystems. The robot design on the left is a hexapod (six-legged)-based flight capable design; the design on the left is a myriapod (many-legged)-based design intended to carry greater payload.

The attractive properties of thin-film PZT have led to an increasing interest in commercializing piezo MEMS technologies. Panasonic Corporation is now offering a thin-film PZT based two-axis gyroscope, and several companies are now marketing PZT MEMS inkjet print-heads.[15,16] Numerous types of other PZT MEMS devices have been demonstrated over the last 20 years, and many of these are described in available reviews on piezo MEMS materials and devices.[12,17–19] This article focuses on two specific application areas for PZT MEMS: one represents a nearer term opportunity for commercialization (RF devices) and the other a high-risk but high-payoff, longer term technology (MEMS robotics).

Small-scale robotics

A more recent application area for PZT MEMS is millimeter-scale robotics.[20] The increased dependence on autonomous systems in various military and commercial applications has motivated the miniaturization of such systems. Smaller platforms will likely be less costly, more portable, and reduce logistical overheads. Extreme miniaturization to the millimeter-scale could provide further benefits in defense applications, including achieving unprecedented levels of stealth and the unique ability to access locations at that scale. In addition, microelectronic and MEMS technologies will permit low-cost manufacturing of these platforms with high levels of integration featuring diverse component functionality (see **Figure 1**). This will also make it possible, with a modular approach to system design, to field larger and more capable heterogeneous networks of robots.

Of course, numerous technical challenges must be overcome to realize this potential. One key challenge is to achieve mobility that is comparable to insects while supporting weight that permits useful system capabilities. For example, for the leg designs of the notional systems illustrated in Figure 1 to achieve the same range and type of motion as insects requires the robot to carry less weight. Supported weight translates to available power and payload capability. Higher performance actuators alleviate this design tradeoff. The capacity of PZT MEMS actuators to generate large displacements and forces efficiently and at low operating

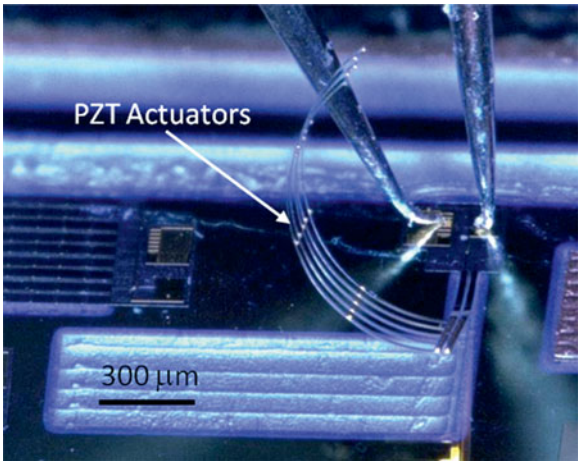


Figure 2. Lead zirconate titanate microelectromechanical systems (PZT MEMS) actuator exhibiting approximately 150° angular displacement (~950 μm) at 15 V. The test structure is 1.5 mm long and consists of 0.5-μm-thick PZT (52/48) on 1 μm of SiO_2.

https://doi.org/10.1557/mrs.2012.269 Published online by Cambridge University Press

voltages uniquely positions the technology to meet this as well as other challenges presented by millimeter-scale robotics.

Actuators

While millimeter-scale autonomous robots may seem like a futuristic concept, the current development of piezo MEMS technologies will enable such systems in the next few years.[21] PZT MEMS actuators exhibit large work and power densities with superior power efficiency relative to electrostatic, magnetic, and electrothermal MEMS actuation approaches.[22] High power efficiency, intrinsic to piezoelectric transduction, is essential for small-scale robotic applications where available power is a central issue. Additionally, low voltage operation alleviates the challenge of efficient small-scale power conversion.[23] Perhaps most importantly though is the ability of thin-film PZT MEMS actuators to produce very large forces and displacements. For example, the test structure in **Figure 2** achieves approximately 150° angular displacement (~950 μm) at 15 V while consuming less than 1 pW of dc power. Currently, this performance is only achievable with PZT MEMS actuation.

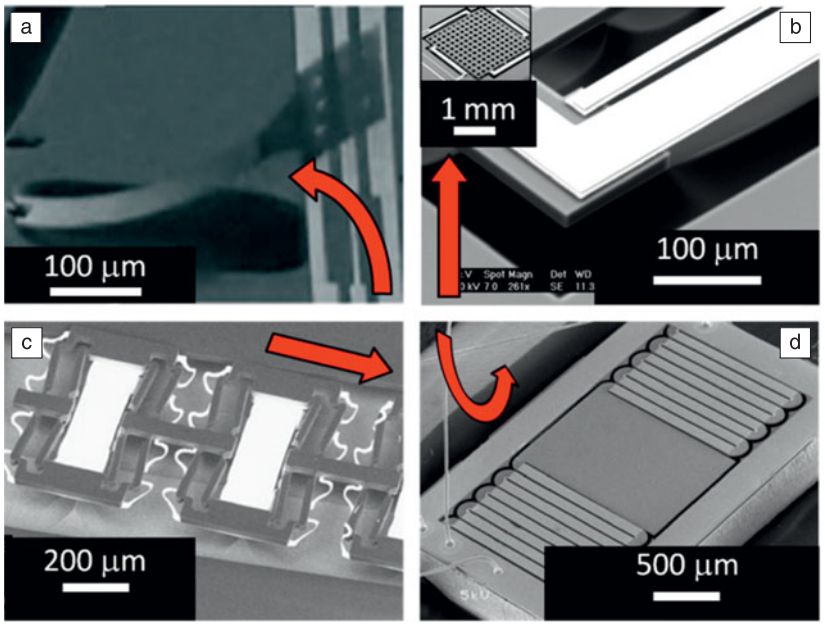


Figure 3. Scanning electron micrographs of example lead zirconate titanate microelectromechanical systems (PZT MEMS)-based actuator designs, including (a) a standard vertical unimorph cantilevered piezo MEMS actuator,[20] (b) a vertical translational unimorph actuator design and complete actuator platform (inset),[24] (c) a lateral (in-plane) actuator,[26] and (d) an out-of-plane rotational actuator design.[29] The red arrows indicate the direction of motion.

In contrast to many other actuator technologies, most piezo MEMS actuators feature very simple geometric designs that easily accommodate various displacement amplification schemes. The most ubiquitous of these amplification designs in MEMS is the unimorph "bender." This structure utilizes the in-plane piezoelectrically induced stress, based on the $e_{31,f}$ piezoelectric constant, to create a moment about the neutral axis of the structure to produce flexural displacements. The unimorph converts the large force/small displacements of the piezoelectric layer into smaller forces/larger displacements of the overall structure. This basic configuration has been exploited to achieve various piezo MEMS actuator designs that are applicable to small-scale robots.

Millimeter-scale robots with the range of motion and dexterity of insects will require joint and leg designs similar in structural complexity. This has partly motivated the development of PZT MEMS actuators that can translate and rotate in and about the three fundamental spatial dimensions. **Figure 3** illustrates some of the basic piezo MEMS actuator designs that have been developed. Vertical displacements, necessary for the lifting of robotic legs, can be achieved through bending of a vertical unimorph cantilever design (Figure 3a) or through pure vertical translation (Figure 3b) with the design described in Reference 24. In-plane motion can be achieved with PZT MEMS lateral actuators (Figure 3c);[25–27] these devices typically use external flexures (springs) to also produce in-plane rotation. The cascading of the actuators can produce the large in-plane rotations desired for robotic joints.[28] Pure out-of-plane rotational actuators (Figure 3d), also based on the simple unimorph, have been developed and can enable more complex robotic joint motions.[20,29] Preliminary results have been achieved with three degrees of freedom millimeter-scale leg designs that are based on the integration of some of these actuators (**Figure 4**).[30] However, significant challenges remain in this area, including achieving true biological-like range of motion and dramatic improvements in the load-bearing capability of these robotic joints.

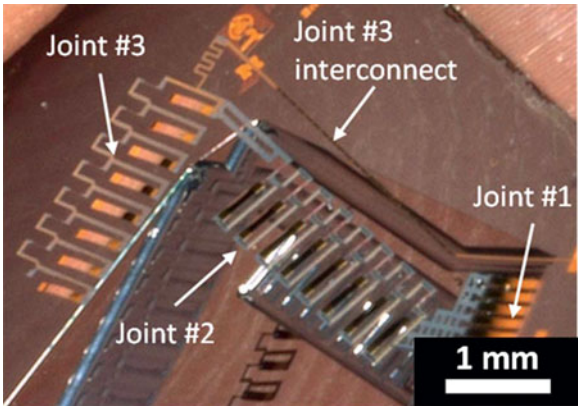


Figure 4. Micrograph of lead zirconate titanate microelectromechanical systems (PZT MEMS) three degrees-of-freedom robotic leg design based on the work in Reference 28. Joint #1 is a vertical unimorph actuator, and joints #2 and #3 are series cascaded lateral actuators.

https://doi.org/10.1557/mrs.2012.269 Published online by Cambridge University Press

Ultrasonic motors

Non-contact, flexure based actuators are not the only class of piezo MEMS actuators applicable to millimeter-scale robotics. One of the earliest papers to discuss insect-scale autonomous robots[31] described the need for thin-film PZT based ultrasonic motors, which utilize vibrations at frequencies above the audible range to create motion. Traveling wave ultrasonic motors (TWUMs) based on bulk PZT have been successfully commercialized for a variety of applications, including auto focus cameras and biomedical instruments.[32] Further miniaturization beyond the tens to hundreds of millimeters in diameter of current TWUMs is attractive because they offer a low power, compact mechanism to achieve large torques at low speeds without gears, while also providing a holding torque with no power input.[33] Despite these benefits, millimeter-scale TWUMs have not been realized because the traditional manufacturing methods are too imprecise. A piezo MEMS approach has enabled high precision structures using photolithographic patterning to create millimeter-scale TWUMs.[34]

These motors operate by exciting a traveling wave in a fixed piezoelectric vibrating component, called the stator. This traveling wave causes the surface of the stator to move in an elliptical pattern. This elliptical surface motion of the stator is then coupled, through the friction provided by a preload normal force, to a rotation in the rotor at the peaks of the traveling wave. The piezo MEMS TWUM described in Reference 34 uses 1-µm-thick PZT (52/48) to excite two out-of-phase standing waves in a 3 mm diameter silicon stator. These standing waves combine through superposition to create a wave of constant amplitude that travels about the disc. To achieve this traveling wave, specific electrode configurations that excite orthogonal vibrational resonant mode shapes are required.

The proof-of-concept TWUM reported in Reference 35, shown in **Figure 5**, consists of two components: a center-fixed stator with thin-film PZT drive actuators and a silicon rotor created using deep reactive ion etching. Although a silicon rotor was used for the proof of concept, the rotor material can be a free parameter, determined either by device optimization or application requirements. Gold wires that are bonded in the center of the stator disc provide electrical signals but also laterally confine the rotor motion. The proof of concept motor exhibits the low power capabilities of the motor (<10 mW), while also demonstrating rotational speeds up to 2300 RPM. Bulk ultrasonic motors typically consume power in the low Watts range and operate in the 100s of RPM.[32] Figure 5b illustrates the measured motor speed and power consumption of the proof of concept motor. The direction of rotation can be reversed by switching the phase offset of the two drive signals and occurs within approximately 30 ms. The key remaining challenge for piezo MEMS enabled TWUMs is the wafer-scale integration of preloaded rotors and torque coupling mechanisms. While thin-film TWUMs have a number of potential applications beyond mobile robotics, the promising results from this early motor suggest such devices are a potential technology for small-scale rotorcraft and large angle robotic joints.

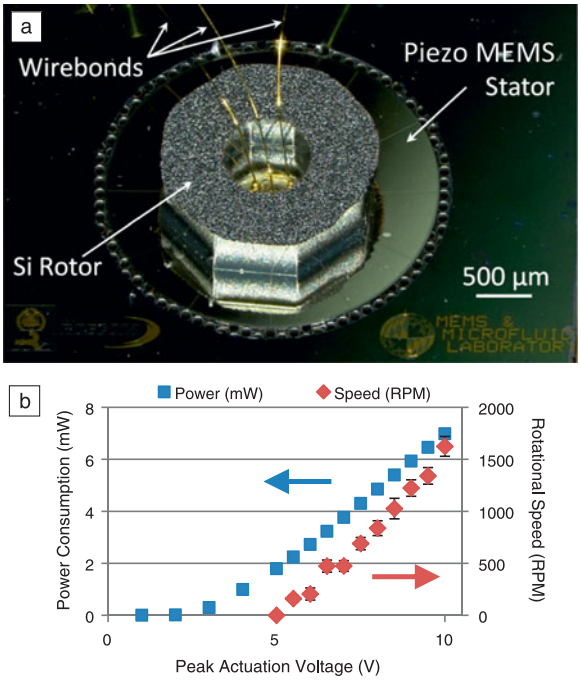


Figure 5. (a) Micrograph of the proof of concept microelectromechanical systems traveling wave ultrasonic motor. (b) Power consumption and rotational speed as a function of peak actuation voltage shows the low-power, low-voltage capabilities of the proof-of-concept system. Error bars on speed represent standard deviation.[35] Note: RPM, revolutions per minute.

Insect-inspired flight

PZT actuators are an enabling mobility technology for airborne as well as terrestrial robots. Researchers have demonstrated the use of bulk PZT piezoelectric actuators to generate lift in centimeter-scale insect-inspired flapping wing robots.[36] These devices, as with flapping wing insects, produce lift by exploiting unsteady aerodynamic effects associated with complex multiple degrees of freedom wing motion. Utilizing bulk piezoelectric material necessitates the use of a mechanical transmission to convert the very large forces and small displacements of the bulk actuator to the required large displacements of the wing.[37] In contrast, the use of thin-film PZT piezo MEMS allows the large wing displacements to be produced directly.[38] Previous work has demonstrated the use of thin-film PZT MEMS actuators to directly drive the stroke (or flapping) and pitch (or rotation) degrees of freedom at angular displacements that are comparable to what insects utilize to fly.[39] The design shown in **Figure 6** includes two orthogonal PZT MEMS unimorph cantilever actuators that independently actuate the stroke and pitch degrees of freedom of the attached microfabricated two millimeter long wing. The Au venation pattern stiffens the wing to allow higher frequency (and hence higher lift) resonant operation of the stroke actuator. These thin-film devices using ~0.5 µm PZT (52/48) thin films have demonstrated 120° of stroke amplitude at 20 V

https://doi.org/10.1557/mrs.2012.269 Published online by Cambridge University Press

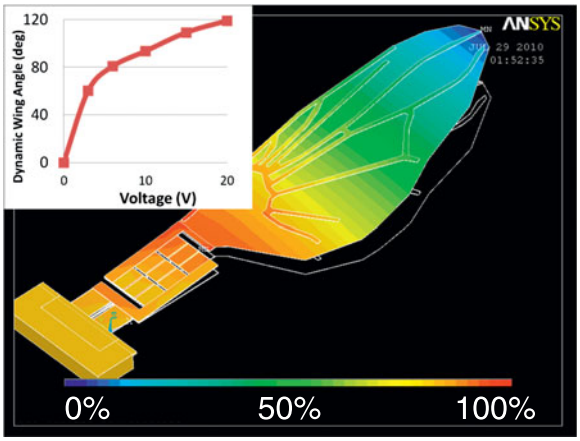


Figure 6. Image of finite element modal analysis of desired vibrational mode of wing and actuators with inset showing measured dynamic stroke amplitude versus voltage based on the work in Reference 39. The displacement is plotted in % of peak displacement.

(see Figure 6 inset) and 45° of pitch amplitude at 20 V at biologically comparable frequencies.

Aerodynamic lift has been achieved with the designs from Reference 39. **Figure 7** shows a test platform consisting of two wings attached to a thin-film body structure that is suspended from a silicon chip with an integrated micro-fabricated tether. The tether provides both the mechanical support and the electrical interconnects needed to actuate the device. When the wing actuators are driven at small displacements, the structure merely vibrates. However, when operated at the intended resonant frequency, the generated aerodynamic lift causes the structure to statically displace vertically. The lift was extracted from the measured displacements and the suspension's finite element modeled spring constant and was determined to be 0.4 μN. This compares well to the expected aerodynamic lift of 0.5 μN, based on quasi-steady aerodynamic models that explain insect flight.[40] While these force values and the corresponding supported mass are quite modest, the validated models predict system-viable millimeter-scale flapping wing robots with previously demonstrated performance and slightly larger wing designs. It is expected that such a PZT MEMS approach could enable 30 mg robots that could fly up to an hour on thin-film battery power alone.[21] Numerous technical challenges, such as the integration of power and control, must be overcome to realize such systems, but the next key milestone will be the demonstration of untethered flight.

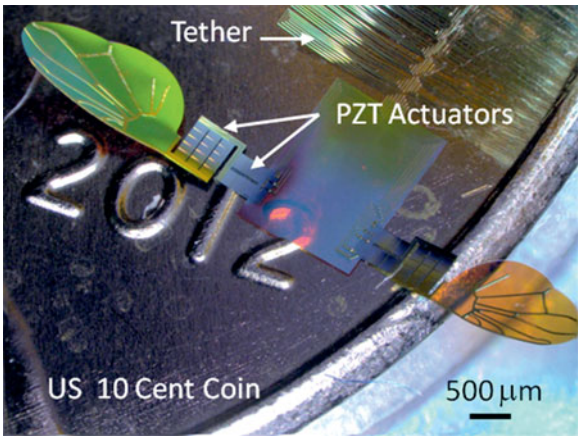


Figure 7. Optical micrograph of a millimeter-scale flapping dual-wing test platform atop a US 10 cent coin; based on the work in Reference 39. This structure utilized integrated lead zirconate titanate microelectromechanical systems (PZT MEMS) actuators to successfully achieve aerodynamic lift. Each wing is approximately 2 mm long. A mechanical/electrical tether supports the structure from a silicon die.

Radio frequency and electronic devices

The development of many RF systems today (cell phones, radios, and radar) is driven by the challenging requirement to simultaneously realize higher performance, increased functionality, and reduced system cost. In many cases, piezo MEMS RF devices can uniquely meet the demand for higher performance and higher levels of integration.[41] The low-voltage and large force/displacement capability of PZT MEMS actuators enable very high performance switches. The attributes are so significant that further miniaturized PZT MEMS switches are being developed for low power mechanical logic applications in addition to RF switching. Another issue facing RF systems is the continued growth of wireless technologies that exacerbates the crowding of the RF spectrum. Consequently, future RF communication systems will likely rely on greater numbers of integrated high selectivity filter banks. The large electromechanical coupling factors of thin-film PZT and the integration potential of MEMS allows for numerous compact and monolithically integrated high performance and wide bandwidth filters on the same chip. Moreover, the large coefficients of PZT thin films have led to new MEMS resonator applications such as high power density electromechanical power converters.[42]

RF MEMS switches

The RF switch or relay is fundamental to most RF circuits and systems. RF MEMS switches have been of interest for their low insertion loss, low power consumption, and high linearity. Commercially available switches/relays from Radant MEMS,[43] WiSpry,[44] Omron,[45] and a few others all utilize electrostatic actuation for their operation with operating voltages in excess of 30 volts. PZT-based piezo MEMS relays offer several advantages over those available currently, including large contact and restoring forces, while maintaining high RF isolation and low actuation voltages that are commensurate with available control voltages.

Switches based on PZT MEMS actuators have been under development for the past decade, with most efforts utilizing unimorph cantilever actuators to provide the physical displacement of a contact pad to open/close the relay.[46–49] Earlier research demonstrated that piezo MEMS switches can be fabricated,

https://doi.org/10.1557/mrs.2012.269 Published online by Cambridge University Press

operated at voltages as low as a few volts, operate consistently across a wide temperature range, and achieve both low insertion loss and high isolation from dc to 10s GHz. Furthermore, individual PZT RF MEMS single input (pole), 4 output (throw) switches were integrated with liquid crystal polymer substrates to demonstrate an extremely compact, low loss phase shifter.[50]

However, these devices exhibited limited cycle reliability. This is due in part to the limited reported data on switches integrated with hermetic packaging technologies. The other key factor was the limited contact force and restoring forces generated in these devices, typically less than 50 μN for each. More recently, design optimization has resulted in the change from an elastic layer using combinations of SiO_2 and Si_3N_4 to single crystal silicon to using thicker films for both the elastic layer and PZT layers. These changes were implemented while maintaining many of the attractive aspects of the early switch design and performance parameters, including actuation voltage, device size, and temperature stability. Recent publications[51,52] have reported switches with 700 μN contact and restoring forces with unpackaged cycle lifetimes exceeding 100 million cycles before the onset of a single failure. These cycle lifetimes compare well with those previously reported in the literature for other unpackaged MEMS switches. A hermetic package is required for final device operation in the millions or billions of cycles depending on final application of use.

An example PZT MEMS RF shunt switch is shown in **Figure 8**a. The actuators, which lie in the gap of a co-planar waveguide transmission, bend upward upon application of a voltage resulting in the RF signal being shunted to ground via electrical traces that reside on the outside of the actuators. This device exhibits an insertion loss of less than 0.3 dB from dc to 20 GHz in the open state, while achieving better than 20 dB of isolation across that same frequency band in the closed state (~15V) (see Figure 8b).

For PZT-based switches, continued improvements to both series and shunt switches and integration with high performance packaging will result in a technology that is attractive for many RF systems. Recently, Advantest has announced the pending release of a piezo MEMS RF relay that would be the first commercially available relay using piezoelectric actuation.[53] The ability to simultaneously achieve low voltage operation and high contact/restoring forces enables a switch technology that can be easily inserted into cellular phones for mode switching, phase shifters for phased array radar systems, and relays for automated test equipment.

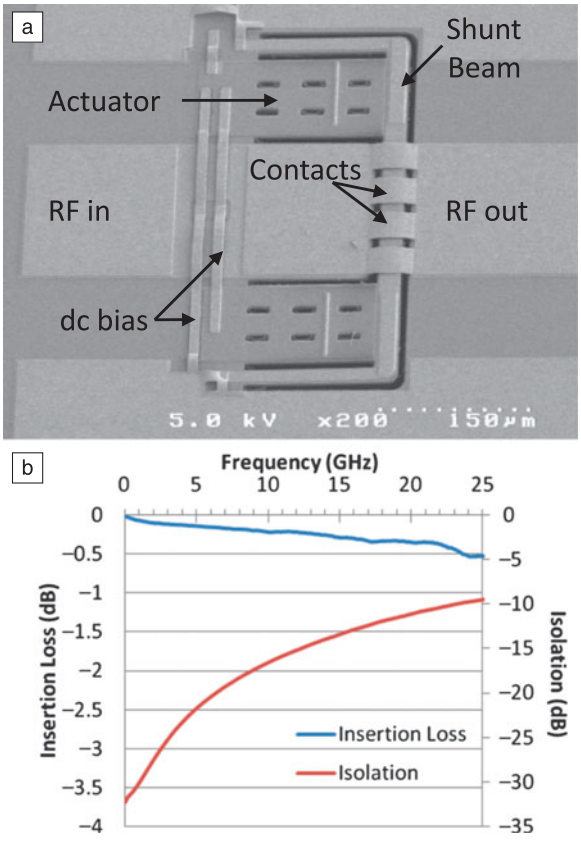


Figure 8. (a) Scanning electron micrograph of a lead zirconate titanate radio frequency (RF) microelectromechanical systems shunt switch and (b) plot of switch insertion loss and isolation.[51]

Mechanical logic

The demand for improved battery lifetimes and further miniaturization of portable consumer electronics is encouraging the development of more energy efficient technologies. For digital

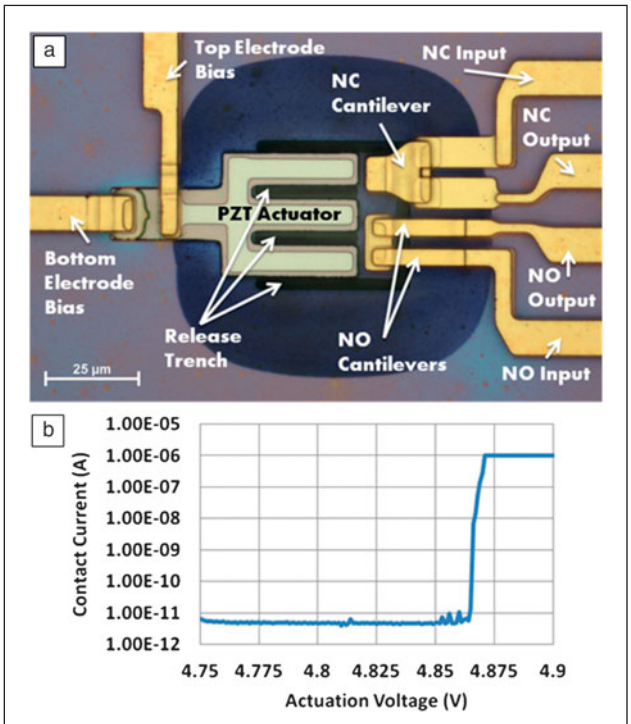


Figure 9. (a) Optical micrograph of the mechanical logic relay indicating the two states of operation and (b) current–voltage characteristics demonstrating a sub-2 mV/decade slope during the switching event.[56] A 1 μA current limit was used for the measurement. Note: NO, normally open; NC, normally closed.

https://doi.org/10.1557/mrs.2012.269 Published online by Cambridge University Press

circuits, the ultimate in low power integrated circuits is achieved through a subthreshold mode of operation (allows for low voltage) at the cost of reduced speed. Additionally, as devices continue to scale to smaller dimensions and attempt to maintain acceptable on-state drain current levels, static power has significantly increased to the point where it is now comparable to the dynamic power consumed.[54]

Relative to conventional metal oxide semiconductor field-effect transistors (MOSFETs), an alternative approach to minimizing energy per operation is to utilize mechanical relays to enable zero static power consumption (i.e., off-state power). The first demonstration of MEMS mechanical logic, digital logic elements realized entirely with MEMS relays, used PZT thin-film cantilever actuators to realize a series of logic units, including an inverter, a NAND (Not AND) gate, and a ring oscillator.[55] More recently, a PZT MEMS single-pole, double-throw relay was developed.[56] The relay, shown in **Figure 9**a, uses PZT vertical unimorph actuators to control two sets of complementary electrical contacts: a normally open and a normally closed contact set. When open, a contact set has an air gap—nominally 200 nm—separating the contacts and preventing the flow of parasitic leakage currents. When closed, a low resistance Au-to-Ru (or RuO_x) contact forms.

From a dynamic power perspective, the low resistance contacts, coupled with large displacements by the PZT actuator, enable turn-on current–voltage (*I–V*) slopes significantly sharper than those achievable by MOSFETs. Measured results, shown in Figure 9b, indicate that the slope is less than 2 mV/decade (compared to 60 mV/decade for MOSFETs[57]). Additionally, due to the large air gap that eliminates leakage in the off-state, the switching voltage to achieve an on-state current to off-state current ratio of 10^5 is about a third of the 300 mV in a theoretically optimal MOSFET device.[57] Static power consumption similarly benefits from the PZT-enabled relays. When the normally closed contact is closed, no voltage is required, which completely eliminates actuator leakage in that state. The result is a relay that is over three orders of magnitude lower in leakage than any CMOS technology node.

Devices have demonstrated dynamic switching energies of 500 fJ per relay per transition and propagation delays of under 100 ns.[56] Measurements showed that the relays were operational from −55°C to 125°C, capable of handling up to 40 V hot-switched across their contacts, and have unpackaged cycling lifetimes over 10^7 cycles in lab air. Fabricated devices have been used to realize all of the logic elements (e.g., combination logic, memory, and an analog to digital interface) necessary to create a complete MEMS microcontroller. One such example, the clock signal generation circuit, is shown in **Figure 10**. This type of circuit is composed of a free-running relaxation oscillator that is then "restored" to a square wave via a buffer element. Ongoing efforts are focused on integrating larger scale circuit elements to demonstrate low power, radiation tolerant, and mechanical microcontroller technology.

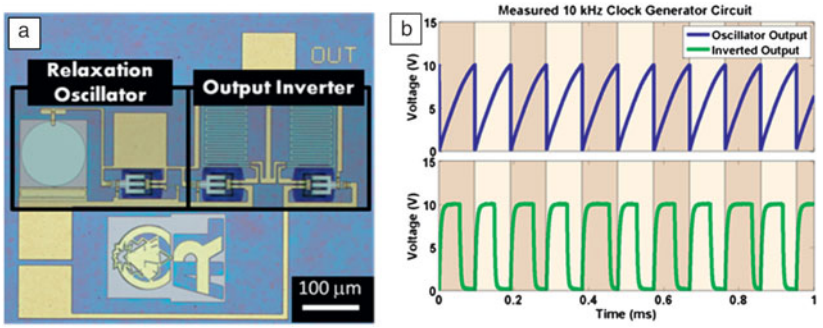


Figure 10. (a) Optical micrograph of a mechanical logic clock generation circuit. (b) Measured results showing a 10 kHz clock signal generated from a fixed, dc input.[56]

Resonators

Although PZT has had a long and successful history as a bulk material for ceramic resonators,[2] there are challenges associated with its use in high frequency resonant devices for RF communication applications. These include mechanical and dielectric losses at high frequencies as well as the temperature stability of the dielectric, ferroelectric, and piezoelectric properties. PZT was explored as a possible film bulk acoustic resonator transducer material;[58] but at the time, the lower mechanical losses in AlN outweighed the advantages of stronger coupling. Despite these challenges, the strong piezoelectric properties and high electromechanical coupling factors enable both wide-bandwidth and low-motional resistance resonators.

Additionally, the high-field ferroelectric response permits the switching-on and -off of the resonant response as well

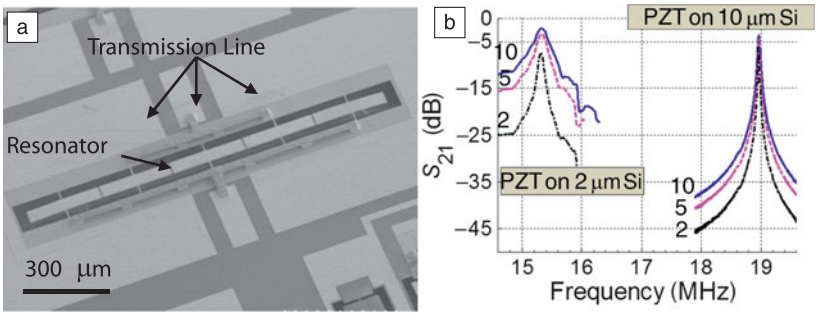


Figure 11. (a) Scanning electron micrograph of a two-port, 5th order length-extensional, 15-MHz lead zirconate titanate resonator and (b) the 50-Ω terminated, forward transmission coefficient, S_{21}, of the resonator under 2, 5, and 10 volt dc biases on both ports.[60] The frequency responses for the 0.5 μm lead zirconate titanate (PZT)(52/48) on 2 and 10 μm of silicon devices are shown.

https://doi.org/10.1557/mrs.2012.269 Published online by Cambridge University Press

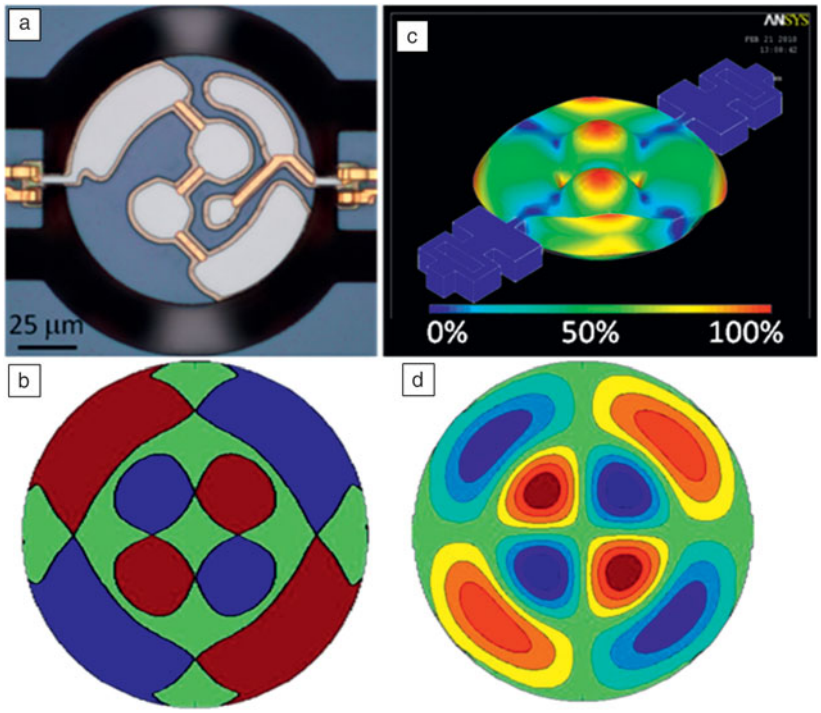


Figure 12. Example disc resonator electrode shaped for a high order out-of-plane flexure mode.[63] (a) Optical micrograph of fabricated device; (b) predicted excitation electrode shape; (c) finite element analysis modal analysis plotting the vector sum of displacements (blue indicates zero displacement and values represent % of peak displacement); and (d) predicted detection electrode shape.

as frequency trimming needed to overcome process-induced device variations. The mechanical losses of the PZT can also be mitigated by the introduction of a high-quality factor material such as silicon; though the introduction of such a high-Q (Q is the quality factor) material poses a trade with the device electromechanical coupling factor and, therefore, ultimate filter bandwidth.

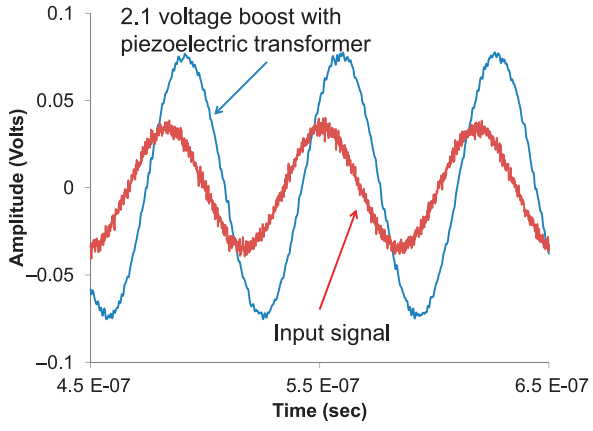


Figure 13. Measured time-domain response of a 15 MHz lead zirconate titanate electromechanical transformer exhibiting a 2.1:1 ac:ac voltage boost.[59]

Work is ongoing to exploit the strong piezoelectric properties of PZT, and a number of advances have been made with PZT-on-silicon RF-MEMS resonators.[59] A low insertion loss of 2.1 dB and very low motional resistance (8 Ω) was recently demonstrated in a device using 0.5 µm PZT(52/48) on 2 µm Si at 15 MHz (see **Figure 11**).[60] Tunable PZT-resonator notch filters, which remove particular frequencies instead of only passing those frequencies as with a typical "pass-band" filter, have achieved rejection levels exceeding 109 dB through current cancellation techniques.[61] Additionally, PZT resonators and PZT switches were monolithically integrated in one of the first all-RF-MEMS switchable filter banks.[62] Furthermore, recent advances in numerical modeling and design have enabled, for the first time, the use of arbitrary vibrational modes in arbitrary resonator geometries by determining the proper electrode designs (see **Figure 12**).[63] With this technique, a low insertion loss of −6 dB at 70 MHz was demonstrated in a disc resonator using 0.5 µm PZT (52/48) on 10 µm Si driven in a harmonic of an out-of-plane flexure mode; a mode previously unexplored in MEMS due to the assumed high losses across all frequencies. This device achieves the same insertion loss as commercially available surface acoustic wave SAW resonators at the same frequency but is several hundred times smaller. These devices are used in a variety of applications, including signal filtering in RF circuits.

One promising application of thin-film PZT-on-silicon resonators is as resonant transformers, as the energy storage element in high-frequency-switched-mode power supplies.[42] Since the conception of the Rosen-type transformer,[64] the first piezoelectric transformer design, bulk piezoelectric transformers have proven to be advantageous over their magnetic counterparts in size, weight, and the absence of electromagnetic interference.[65] Though high electromechanical coupling is desired for a number of reasons, including high power factors in ac:ac transformer circuits, the added silicon as a structural layer within the thin-film PZT transformer can mitigate mechanical loss and provide higher power densities over thin-film, PZT-only implementations. Recent work has shown thin-film piezoelectric PZT-on-silicon transformers with 2:1 open circuit voltage gain (see **Figure 13**), high efficiency exceeding 60% for the 1:1 transformer case at 15 MHz, and power densities exceeding 1 W/mm^3.[60] Further improvements in power handling and efficiency are required for insertion into full power converters.

Conclusions

The strength and power efficiency of electromechanical coupling in (lead zirconate titanate) PZT-based MEMS

https://doi.org/10.1557/mrs.2012.269 Published online by Cambridge University Press

(microelectromechanical systems) devices has enabled state-of-the-art performance in various actuators and transducers. Thin-film PZT enables large force and displacement generation in piezo MEMS actuators such as (radio frequency) RF switches and ultrasonic motors; efficient transduction in devices such as mechanical logic relays; low voltage operation in actuators such as millimeter-scale robotic wing joints; and low-loss high-coupling in devices such as piezoelectric transformers and RF resonators. PZT MEMS technology is receiving significant attention for RF and small-scale robotic applications for these reasons; however, there are opportunities to exploit these same material and device attributes in many other applications. The next several years will see the continued and expanded development of PZT-based MEMS in these areas as well as in inkjet printer heads, ultrasonic medical imaging, inertial sensors, and energy harvesting.

Acknowledgments

The authors would like to thank their many collaborators, including Drs. Susan Trolier-McKinstry (Pennsylvania State University), Sunil Bhave (Cornell University), Don Devoe (University of Maryland), and Madan Dubey (US Army Research Laboratory). Additionally, the authors thank Brian Power, Joel Martin, and Luz Sanchez for their efforts in piezo MEMS device fabrication.

References

1. K. Uchino, J.R. Giniewicz, *Micromechatronics* (Marcel Dekker, New York, NY, 2003).
2. S. Fujishima, *IEEE Trans. Ultrason. Ferroelectr. Freq. Control* **47**, 1 (2000).
3. M. Kohli, C. Wuethrich, K. Brooks, B. Willing, M. Forster, P. Muralt, N. Setter, P. Ryser, *Sens. Actuators, A* **60**, 147 (1997).
4. K.R. Udayakumar, T.S. Moise, S.R. Summerfelt, K. Boku, K.A. Remack, J. Gertas, A. Haider, Y. Obeng, J.S. Martin, J. Rodriguez, G. Shinn, A. McKerrow, J. Eliason, R. Bailey, G.R. Fox, *Jpn. J. Appl. Phys.* **46**, 2180 (2007).
5. www.ramtron.com/products/nonvolatile-memory.
6. www.ti.com/product/msp430fr5728.
7. www.fujitsu.com/us/services/edevices/microelectronics/memory/fram.
8. F. Gerfers, P.M. Kohlstadt, E. Ginsburg, M. Yuan He, D. Samara-Rubio, Y. Manoli, L.-P. Wang, in *Solid State Circuits Technologies*, J.W. Swart, Ed. (InTech, New York, 2010), pp. 333–352.
9. R. Ruby, P. Bradley, D. Clark, D. Feld, T. Jamneala, W. Kun, in *Proc. MTT-S Int. Microwave Symp. Dig.* (2004), pp. 931–934.
10. www.avagotech.com/pages/en/rf_microwave/fbar_filters.
11. S. Trolier-McKinstry, P. Muralt, *J. Electroceram.* **12**, 7 (2004).
12. P. Muralt, R.G. Polcawich, S. Trolier-McKinstry, *MRS Bull.* **34**, 658 (2009).
13. F. Calame, P. Muralt, *Appl. Phys. Lett.* **90**, 062907 (2007).
14. A.H. Meitzler, H.F. Tiersten, A.W. Warner, D. Berlincourt, G.A. Coquin, F.S. Welsh III, *ANSI/IEEE Stand.* 17 (1987).
15. www.epson.com/cgi-bin/Store/Landing/InkTechPrinter.jsp.
16. www.fujifilmusa.com/products/industrial_inkjet_printheads/technology/mems/index.html.
17. P. Muralt, *J. Am. Ceram. Soc.* **91**, 1385 (2008).
18. S. Tadigadapa, K. Mateti, *Meas. Sci. Technol.* **20**, 092001 (2009).
19. R.G. Polcawich, J.S. Pulskamp in *MEMS Materials and Processes Handbook, 1st ed.*, R. Ghodssi, P. Lin, Eds. (Springer, New York, 2011), pp. 273–344.
20. J.S. Pulskamp, R.G. Polcawich, K. Oldham, in *Proc. ASME 2009 IDETC/MNS* (2009), p. 797.
21. J.S. Pulskamp, in *Proc. SPIE* 8373 (2012).
22. K. Oldham, J. Pulskamp, R. Polcawich, P. Ranade, M. Dubey, *Integr. Ferroelectr.* **95**, 54 (2007).
23. B. Morgan, S. Bedair, J.S. Pulskamp, R.G. Polcawich, C. Meyer, C. Dougherty, X. Lin, D. Arnold, R. Bashirullah, R. Miller, M. Roosz, *Proc. SPIE* **7679**, 76790V–1 (2010).
24. Z. Qiu, J.S. Pulskamp, X. Lin, C.-H. Rhee, T. Wang, R.G. Polcawich, K. Oldham, *J. Micromech. Microeng.* **20**, 1 (2010).
25. K. Oldham, J.S. Pulskamp, R.G. Polcawich, M. Dubey, *J. Microelectromech. Syst.* **17**, 890 (2008).
26. N.J. Conway, A.J. Traina, S.-G. Kim, *J. Micromech. Microeng.* **17**, 781 (2007).
27. Y.H. Seo, D.-S. Choi, J.-H. Lee, T.-J. Je, K.-H. Whang, *Sens. Actuators, A* **127**, 302 (2006).
28. B. Edamana, B. Hahn, J.S. Pulskamp, R.G. Polcawich, K. Oldham, *IEEE/ASME Trans. Mechatron.* **16**, 884 (2011).
29. M. Tani, M. Akamatsu, Y. Yasuda, H. Toshiyoshi, in *Proc. IEEE MEMS* (2007), p. 699.
30. K. Oldham, C.-H. Rhee, J.-H. Ryou, R.G. Polcawich, J.S. Pulskamp, in *Proc. ASME 2009 IDETC/MNS* (2009), p. 759.
31. A. Flynn, L.S. Tavrow, S.F. Bart, R.A. Brooks, D.J. Ehrlich, K.R. Udayakmar, L.E. Cross, *J. Microelectromech. Syst.* **1**, 1 (1992).
32. S. Ueha, Y. Tomikawa, *Ultrasonic Motors: Theory and Applications* (Oxford University Press, New York, 1993).
33. K. Uchino, *Smart Mater. Struct.* **7**, 273 (1998).
34. G.L. Smith, R.Q. Rudy, R.G. Polcawich, D.L. Devoe, *Sens. Actuators, A* (2011), doi:10.1016/j.sna.2011.12.029.
35. R.Q. Rudy, G.L. Smith, D.L. DeVoe, R.G. Polcawich, 2012 Solid State Sensor, Actuator and Microsystems Workshop (Hilton Head, SC, 2012), June 3–7, 2012, pp. 417–420.
36. R.J. Wood, *IEEE Trans. Rob.* **24** (2), 341 (2008).
37. S. Avadhunula, R.J. Wood, D. Campolo, R.S. Fearing, in *Proc. IEEE Int. Conf. Rob. Autom.* (2002), p. 52.
38. J. Bronson, J.S. Pulskamp, R.G. Polcawich, C. Kronigner, E. Wetzel, in *Proc. IEEE MEMS* (2009), p. 1047.
39. J. Pulskamp, G. Smith, R. Polcawich, C. Kroninger, E. Wetzel, in *Proc. 2010 Solid State Sensor, Actuator and Microsystems Workshop* (2010), p. 390.
40. C.P. Ellington, *J. Exp. Biol.* **202**, 3439 (1999).
41. G. Piazza, P.J. Stepanou, A.P. Pisano, *J. Microelectromech. Syst.* **15**, 1406 (2006).
42. S. Bedair, J. Pulskamp, B. Morgan, R. Polcawich, in *Proc. Power MEMS 2009* (2009), pp. 435–439.
43. www.radantmems.com/radantmems/switchoverview.html.
44. www.wispry.com/technology.php.
45. www.components.omron.com/components/web/webfiles.nsf$FILES/family.html?ID=DSAX-7LARFC.
46. S.J. Gross, S. Tadigadapa, T.N. Jackson, S. Trolier-McKinstry, Q.Q. Zhang, *Appl. Phys. Lett.* **83**, 174 (2003).
47. H.-C. Lee, J.-H. Park, J.-Y. Park, H.-J. Nam, J.-U. Bu, *J. Micromech. Microeng.* **15**, 2098 (2005).
48. R.G. Polcawich, J.S. Pulskamp, D. Judy, P. Ranade, S. Trolier-McKinstry, M. Dubey, *IEEE Trans. Microwave Theory Tech.* **55**, 2642 (2007).
49. R.G. Polcawich, D. Judy, J.S. Pulskamp, S. Trolier-McKinstry, M. Dubey, *IEEE MTT-S Microwave Symp.* (2007), p. 2083.
50. D.J. Chung, R.G. Polcawich, D. Judy, J. Pulskamp, J. Papapolymerou, *IEEE MTT-S Microwave Symp.* (2008), p. 21.
51. T.G. Ivanov, J.S. Pulskamp, R.G. Polcawich, R.M. Proie, *IEEE MTT-S Microwave Symp.* (2012), in press.
52. T.G. Ivanov, R.M. Proie, J.S. Pulskamp, R.G. Polcawich, A. Zaghloul, *Solid State Sensor, Actuator and Microsystems Workshop* (Hilton Head Island, SC, 2012), p. 389.
53. www.advantest.co.jp/news/press-2011/20120319/en-index.shtml.
54. International Technology Roadmap for Semiconductors (ITRS, 2000–2007); www.itrs.net/reports.html.
55. D.C. Judy, R.G. Polcawich, J.S. Pulskamp, *Solid State Sensor, Actuator and Microsystems Workshop* (Hilton Head Island, SC, 2008), p. 328.
56. R.M. Proie, R.G. Polcawich, J.S. Pulskamp, T. Ivanov, M.E. Zaghloul, *J. MEMS* **20**, 1032 (2011).
57. G. McFarland, M. Flynn (Tech. Rep. CSL-TR-95–662, Stanford University, 1995).
58. J.D. Larson, S.R. Gilbert, B. Xu, in *Proc. IEEE Ultrasonics Symp.* (2004), p. 173.
59. J.S. Pulskamp, S.S. Bedair, R.G. Polcawich, D. Judy, S.A. Bhave, in *Proc. IEEE Freq. Control Symp.* (2011), p. 1.
60. S.S. Bedair, J.S. Pulskamp, R.G. Polcawich, D. Judy, A. Gillon, S. Bhave, B. Morgan, in *Proc. IEEE MEMS* (2012), p. 708.
61. S.S. Bedair, D. Judy, J. Pulskamp, R.G. Polcawich, A. Gillion, E. Hwang, S. Bhave, *Appl. Phys. Lett.* **99**, 1 (2011).
62. J.S. Pulskamp, D.C. Judy, R.G. Polcawich, R. Kaul, H. Chandrahalim, S.A. Bhave, in *Proc. IEEE MEMS* 900 (2009).
63. J.S. Pulskamp, S.S. Bedair, R.G. Polcawich, G.L. Smith, J. Martin, B. Power, S.A. Bhave, *IEEE Trans. Ultrason. Ferroelectr. Freq. Control* **59**, 1043 (2012).
64. C.A. Rosen, in *Proc. Electronic Comp. Symp.* (1956), p. 205.
65. A. Carazo, in *Proc. Mater. Res. Soc. Symp.* (2004), p. D1.7.1. □

https://doi.org/10.1557/mrs.2012.269 Published online by Cambridge University Press